Effects of crystal orientation and temperature on the deformation mechanism and mechanical property of Cu nanowire

Weiwei Pang ✉, *Siyuan Yu, Zhijie Lin, Yizhe Zhao, Fuxing Yin*

School of Materials Science & Engineering, Tianjin Key Laboratory of Materials Laminating Fabrication and Interface Control Technology, Hebei University of Technology, Tianjin 300130, People's Republic of China
✉ *E-mail: pangweiwei@hebut.edu.cn*

Published in Micro & Nano Letters; Received on 24th September 2019; Revised on 17th December 2019; Accepted on 6th January 2020

The effects of crystallographic direction and temperature on the deformation mechanism and properties of Cu nanowire (NW) are studied via systematic simulations and theoretical analysis. It is found that the elastic module, yield stress and yield strain are quite different for five oriented NWs. As the crystallographic orientation of NW varies, both the yield stress and the yield strain firstly reduce to the minimum value, then gradually increase. Furthermore, the evolutions of flow stress after yield point are also obviously different for five oriented NWs, which are associated with the plastic deformation mechanisms. With the crystallographic orientation of NW varying, the simulated atomic snapshots show that the dominant deformation mechanism transforms from the shuffling-assisted single dislocation-nucleation to the collective dislocation-nucleation, then to the twinning migration, and finally to the combination of dislocation glide and micro-twinning. According to the normal stress perpendicular to the slip plane and shear stress on the slip plane, the authors theoretically predict the deformation mechanisms for different oriented NWs, which turn to be in good consistent with the authors' observed deformation mechanisms. Besides, they also propose that the temperature effects are different for different oriented NWs.

1. Introduction: In recent years, nanoscale metal materials have attracted extensive interest due to superior mechanical, magnetic and thermal properties [1–4]. Nanowire (NW), as one of the most representative low-dimensional nanostructured materials, has widely used in various fields [5–7]. Therefore, understanding the deformation behaviour of metal NW becomes an essential task for the optimal design and wide application. Especially in engineering applications, NW is often subjected to the loading of various orientations. It is urgent to study the effects of crystal orientations on the deformation behaviour under various loadings.

Recently, a great deal of experiment and simulation studies have performed on investigating the mechanical properties and structural evolutions of metal NW under the bending, compression, tensile loading [8–13]. Seo *et al.* [14] investigated the tensile deformation of Au NW using the high-resolution electron microscopes, and reported that the plastic deformation proceeds layer-by-layer in an atomically coherent fashion. Wen *et al.* [15] analysed the structural evolution of Ni NW at different strain rates, and found a critical strain rate beyond which the atomic structure completely transforms into the amorphous state. Chang *et al.* [16] studied the tensile properties of Ti NW under different strain rates, and presented that the yield stress and fracture strain increase with strain rate. Zhuo and Beom [17] investigated the size effect on the torsional deformation of Si NW, and reported that the deformation mechanism transforms from an amorphous state to dislocation nucleation when the diameter exceeds 7.7 nm. Peng *et al.* [18] studied the fracture mode of Cu NW with the aid of the in situ uniaxial tensile tests, and found that fracture modes dependent on the diameters of tested NWs. Liu and Shen [19] analysed the fracture behaviours of Si NW at low temperature, and reported that the failure responses are shear slip, crystal-to-amorphous transition and cleavage for ⟨110, ⟨100⟩, ⟨111⟩ oriented NW, respectively. Zhu *et al.* [20] explored the orientation dependence of Ni NW deformation under bending loading, presented that the (121) oriented NW uniformly deforms, but the (111) and (010) oriented NWs prefer to locally deform. Sainath and Choudhary [21] investigated the effect of orientation on the deformation behaviour of Fe NW, and reported that the (100), (112) and (102) oriented NWs deform predominantly by twinning mechanism, whereas the (110) and (111) oriented NWs deform by dislocation slip. Wang *et al.* [22] performed in-situ atomic bending experiments on twinned Ni NW, and found that plastic deformation is carried by dislocation to phase transition, and then to grain boundary with increasing bending. Sun *et al.* [23] explored the fracture behaviour of twinned Cu NW under tensile loading, and revealed that the fracture behaviour exhibits a brittle-to-ductile transition with increasing the twin spacing for intermediate-length NW. Sansoz and Dupont [24] studied the processes of spherical indentation in nanocrystalline Ni NW, and presented that plastic deformation is carried by grain boundary sliding. Zhu *et al.* [25] studied the coupled effect of sample size and grain size in polycrystalline Al NW, and presented that different size effects originate from different deformation mechanisms.

According to the available literature, the physical properties and deformation behaviours of metal NW are closely related to the loading strain rate, temperature, loading mode, size, crystal orientation, crystal structure, etc. [26–32]. Although plenty of investigates had been done to study the mechanical behaviour of metal NW, there are still a lot of unclear aspects in accurate modelling. In this Letter, we study the mechanical properties and structural evolutions of different oriented Cu NWs via systematic simulations and rationalised analysis in detail. It is found that the elastic module, the yield stress and strain, the fracture strain are strongly dependent on the crystallographic orientation of the NW. The dominant deformation mechanism transforms from the shuffling-assisted single dislocation-nucleation to the collective dislocation-nucleation, then to the twinning migration, and finally to the combination of dislocation glide and micro-twinning with the crystallographic orientations of NW varying. According to the calculated normal stress and shear stress, we explain the transformation of the deformation mechanism. These findings provide insight into precise modelling.

2. Atomic modelling: In this work, the sample material used is the single-crystal Cu. The embedded atom method potential [33], which can well describe the mechanical properties and structure defect evolution, is used to model the interatomic interaction. The parallel LAMMPS software package is employed for simulation [34]. The x, y, z axes of simulation box are along the [111],

[-1-12], and [1-10] crystallographic orientations, respectively. In order to study the dependence of the deformation behaviour on the crystallographic orientation of NW, we rotate the atoms around the z-axis to 0°, 30°, 60°, 90°, 120°, respectively. To eliminate the size effect, the dimensions of all oriented NWs have the same length of 50 nm × 6 nm × 6 nm, which contain ~1.67×10^5 atoms. The free boundary conditions are used along with the y and z axes. Prior to the tensile deformation, the structures of NWs are first optimised with a conjugate gradient algorithm. Then, it is relaxed at ambient pressure $P = 0$ GPa and temperature $T = 300$ K or 3 K. After equilibration, the thermostat is turned off and the uniaxial tensile strain is applied along the x-axis. The uniaxial tensile strain was carried out in a velocity-controlled method by imposing linearly varying velocity to atoms along the x-axis, and the strain rate is 10^8/s. The common neighbour analysis values [35] are calculated to distinguish the atomistic structures and the software package Open Visualization Tool (OVITO) [36] is used to visualise the evolution configurations.

3. Results and discussion: It is known that stress–strain curve is an important graphical measure for the mechanical properties of NWs. In an experiment, it is obtained from surface velocity measurement and used to evaluate yield stress, fracture strength. The molecular dynamics simulation also provides a complete stress–strain curve. In this Letter, we calculate the stress using the virial theorem. Fig. 1 shows the tensile stress–strain curves for five oriented NWs at temperature $T = 300$ K. It can be seen that all the NWs undergo an initial elastic deformation that is nearly linear until the peak stress value, and then the stress drops abruptly. However, there also are some distinctly different behaviours among the five oriented NWs. On the one hand, the slope of stress–strain curve in the elastic region represents the elastic module, and it is obvious that the elastic moduli are quite different for five oriented NWs, which indicates a close relation of the elastic modulus to the crystallographic orientation. On the other hand, the abrupt stress drop represents the occurrence of plasticity deformation in the NWs. For five different oriented NWs, the incipient plasticity occurs at different stresses and strains, respectively. This phenomenon demonstrates the yield stress and strain are strongly dependent on the crystallographic orientation. For example, both the yield stress and strain are the smallest for the NW rotated 30°. In addition to the above, the evolution behaviours of the stress–strain curves after the yield point are also obviously different for five oriented NWs. Such as, for the NWs rotated 0°, plastic flow stress severely oscillate and the stress–strain curves exhibit saw shape. For the other oriented NWs, the plastic flow stress decreases rapidly after the second peak. Furthermore, we also notice that the fracture strain is very small for the NW rotated 60°. These phenomena of plastic flow stress may result from the different deformation mechanisms, and we will analyse detailed the dependence of deformation mechanism on the crystallographic orientation in the following section.

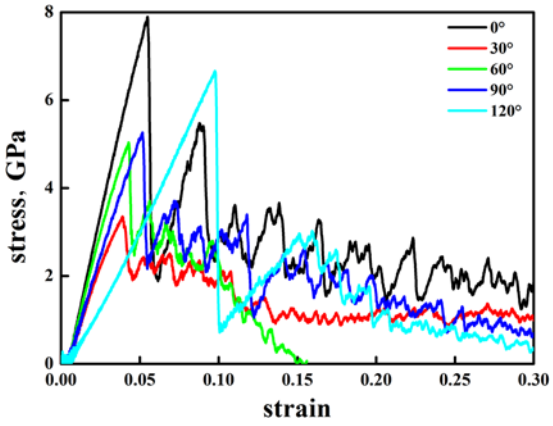

Fig. 1 *Tensile stress–strain curves for different oriented NWs*

In order to further quantitatively analyse the dependence of mechanical properties of NWs on the crystallographic orientations, Fig. 2 shows the yield stress and strain for all oriented NWs at temperature $T = 300$ K. It can be clearly seen from Fig. 2, both the yield stress and strain of NWs strongly dependent on the crystallographic orientations. The yield stress value varies from 7.89 to 3.35 GPa for different oriented NWs and is reduced by 57.5%. As well as, the yield strain varies from 0.0977 to 0.0390 and is reduced by 60%. In addition, the stress and strain curves exhibit the same variation tendency with the variation of NW orientations. The whole curve can be divided into three parts. Firstly, it reduces to the minimum value, in which case the NW rotated 30°. Subsequently, it gradually increases with the variation of NW orientations.

Owing to the fact that these differences in mechanical properties for different oriented NWs result from different deformation mechanisms. Therefore, in this section, we present the snapshots of evolution processes of atomic structures for all oriented NWs, as shown in Fig. 3. Here, the green and red atoms represent face-centred cubic (FCC) and hexagonal close-packed (HCP) structures, respectively. From Fig. 3*a*, it can be seen that the shuffling-assisted single dislocation-nucleation mechanism dominants the deformation process for the NW rotated 0°. Here, the strain corresponding to each snapshot is 0.091, 0.169 and 0.390, respectively. Following the yielding, the single Shockley partial dislocation intermittently initiates from the free surface. Then, it propagates through the NW and disappears at the opposite surface, leaving a slippage step on the surface. This deformation pattern of intermittent nucleation and annihilation of single dislocation is responsible for the saw shape on stress–strain curves. As the tensile loading increases, local atomic lattice structures are completely destroyed by multiple glides of dislocations, which results in the fracture of NW.

In comparison to Fig. 3*a*, the plastic deformation is initially originated via the collective dislocation-nucleation mechanism for the NW rotated 30°, as can be seen in Fig. 3*b*. Here, the strain corresponding to each snapshot is 0.045, 0.157 and 0.424, respectively. It is obvious that multiple parallel Shockley partial dislocations generate on the (111) slip plane with random spatial distribution after yielding. In the subsequent deformation process, the deformation mechanism transforms into the migration of the twinning boundary on the (11-1) slip plane. The twinning boundary interacts with the Shockley partial dislocations on the (111) slip plane, causing the partial dislocation to disappear. The NW is eventually broken by the interaction of dislocations on the two slip planes.

For the NW rotated 60°, as shown in Fig. 3*c*, it can be seen that twinning deformation plays an important role during the tensile process. Here, the strain corresponding to each snapshot is 0.044, 0.046 and 0.115, respectively. After yielding, the twinning embryo on the (111) slip plane forms with the aid of the nucleation

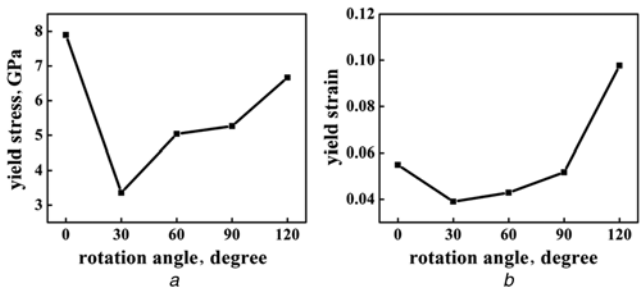

Fig. 2 *Yield stress and strain for different oriented NWs*
a Curve of yield stress versus rotation angle
b Curve of yield strain versus rotation angle

doi: 10.1049/mnl.2019.0559

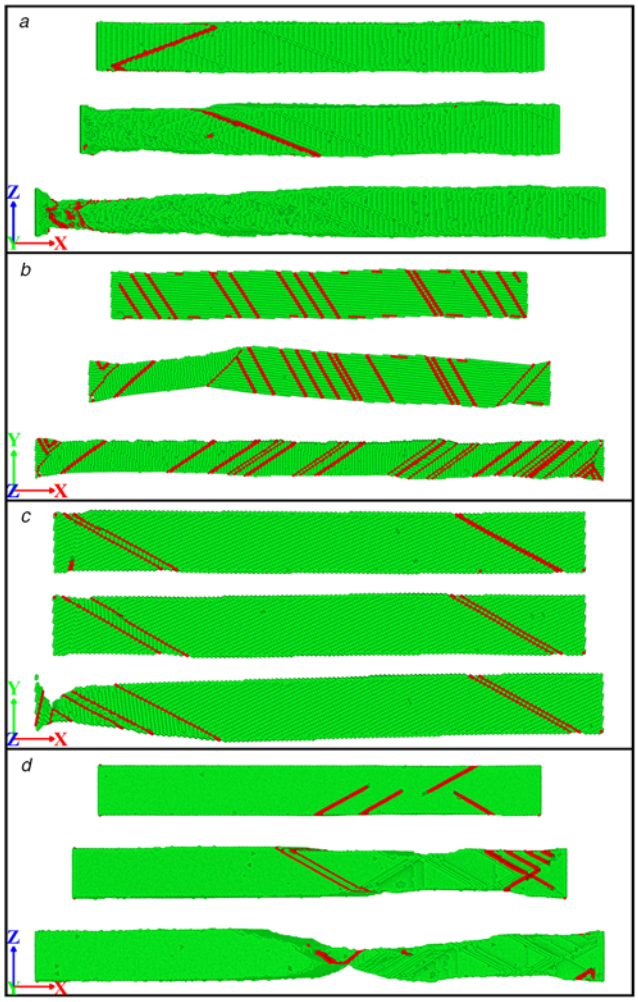

Fig. 3 *Simulation snapshots of atomic structure for all oriented NWs during the tensile process*
a Snapshots for the NW rotated 0°
b Snapshots for the NW rotated 30°
c Snapshots for the NW rotated 60°
d Snapshots for the NW rotated 90°

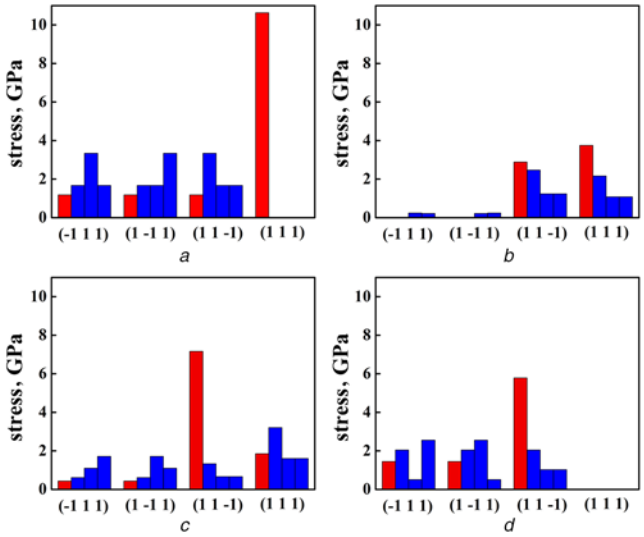

Fig. 4 *Normal stress perpendicular to the slip plane and shear stress on the slip plane for all oriented NWs*
a Calculated stress for the NW rotated 0°
b Calculated stress for the NW rotated 30°
c Calculated stress for the NW rotated 60°
d Calculated stress for the NW rotated 90°

of two partial dislocations on adjacent slip planes. Then, the twin gradually grows in width along the NW axis through the successive nucleation of partial dislocations. Eventually, the migration coupling of two twins on the (111) and (11-1) slip planes gives rise to the fracture of the NW.

In addition, we find that the plastic deformation is carried by multiple glides of dislocations and the formation of a few micro-twins for the NWs rotated 90° and 120°. Fig. 3*d* shows the deformation snapshot for the NW rotated 90°. Here, the strain corresponding to each snapshot is 0.053, 0.174 and 0.350, respectively. In the early stage of plastic deformation, several dislocations on different slip planes intermittently occur on the free surface and glide into the opposite free surface to disappear. With increasing the tensile loading, a few microtwin structures are observed in the NWs. As well as, the NWs finally rupture locally due to the combination of dislocation glide and microtwinning.

To assist in interpreting the simulated snapshots, we calculate the stress components along the glide direction on the slip plane at the first dislocation nucleation moment according to the expression of $|b\cdot\sigma\cdot n|$ for all oriented NWs, as shown in Fig. 4. Here, the red and blue bars represent the normal stress perpendicular to the slip plane and shear stress on the slip plane, respectively. It is observed from Fig. 4, although the normal stress is largest on the (111) slip plane in Fig. 4*a*, the shear stress is zero. Therefore, there is no activated dislocation or twin on this slip plane and Shockley partial dislocation is activated on the other three slip planes, which is consistent with the simulated snapshots. On the other side, it is known that the shear stress needs to exceed a certain value for dislocation nucleation, as well as both the normal stress and shear stress, which must exceed certain values for the twinning migration. By comparing the normal stress and shear stress in Fig. 4, we note that both the normal stress value and shear stress value are lager on the (111) slip plane in Fig. 4*c*, indicating that the stresses on these slip planes are sufficient to activate the twinning migration mechanism. In addition, both the normal stress value and shear stress value are moderate on multiple slip planes in Fig. 4*d*, which leads to the dislocation glide and micro-twin formation dominating the plastic deformation processes.

It is known that the simulation temperature is one of the important factors affecting the material properties. In this work, we also investigated the temperature effects on the mechanical properties of different oriented NWs. Fig. 5 shows the yield stress, yield strain and fracture strain extracted from the stress–strain curves at temperatures 3 and 300 K. It can be seen that both the yield stress and strain decrease with increasing the temperature for all oriented NWs. However, the decreased magnitude varies with the orientation of NWs. Such as, the yield stress value decreases by 38 and 19% for the NWs which rotated 0° and 60°, respectively, which demonstrates the mechanical properties are insensitive to the simulation temperature for the NW rotated 60°. In addition, we also observe that the increase magnitude of yield stress is obviously higher than that of the yield strain, indicating that the yield stress is more sensitive to the simulation temperature.

On the other side, we also analyse the atomic snapshots during the deformation process in detail. It is found that temperature slightly affects the deformation behaviour and does not change the main deformation mechanism. However, the higher the temperature, the more obvious the twinning domination mechanism, which will affect the fracture strain of the NWs, as shown in Fig. 5*c*. For the NWs dominated by dislocation glide mechanism, such as the NW rotated by 0°, the glide speed of dislocations improves as the temperature increases, which results in the fracture strain decreasing. While, for the NWs carried by dislocation glide and microtwin formation mechanism, such as the NW rotated 120°, the twinning mechanism is superior to the dislocation glide mechanism with

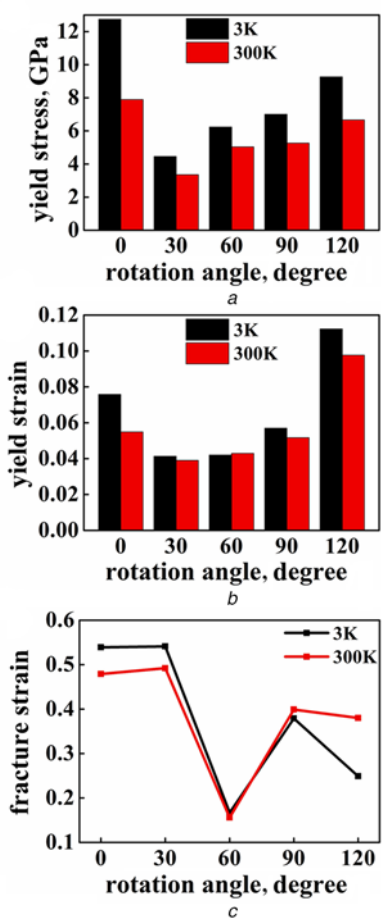

Fig. 5 *Yield stress, yield strain and fracture strain for different oriented NWs at different temperatures*
a Temperature effects on the yield stress
b Temperature effects on the yield strain
c Temperature effects on the fracture strain

the increase of temperature, which leads to hardening and the second peak value going up after yielding point. As a result, the ductility enhances the flow stress and fracture strain increases.

4. Conclusion: In conclusion, through systematic MD simulations and rationalised analysis, we have studied the deformation behaviours of different oriented Cu NWs during the tensile process. It is found that all the NWs undergo a nearly linear elastic deformation up to the peak stress value and then the stress drops abruptly. However, there also are some distinctly different behaviours among the different oriented NWs. On the one side, the elastic module, yield stress and yield strain are quite different for five oriented NWs, which indicate close relations of these physical quantities to the crystallographic orientations. With the variation of NW orientations, both the yield stress and the yield strain firstly reduce to the minimum value, then gradually increase. On the other side, the evolution behaviours of the stress-strain curves after the yield point are also obviously different for five oriented NWs. Such as, for the NWs rotated 0°, plastic flow stress severely oscillate and the stress–strain curves exhibit saw shape. In addition, by comparing these simulated atomic snapshots for different oriented NWs, we find that the plastic deformation modes transform with the variation of NW orientations. For the NW rotated 0°, the shuffling-assisted single dislocation-nucleation mechanism dominants the deformation process. For the NW rotated 30°, the plastic deformation is initially originated via the collective dislocation-nucleation mechanism, and then transforms into the twinning migration mode in the subsequent process. For the NW rotated 60°, twinning deformation plays an important role during the tensile process. For the NWs rotated 90° and 120°, the plastic deformation is carried by multiple glides of dislocations and the formation of a few microtwins. According to the normal stress perpendicular to the slip plane and shear stress on the slip plane, the predicted deformation mechanisms are in good agreement with the observed deformation mechanisms. Besides, we also investigate the temperature effects on the mechanical properties of different oriented NWs, and find that the increase magnitudes of yield stress and strain vary with the orientation of NWs.

5. Acknowledgments: This work was financially supported by the National Natural Science Foundation of China (grant no. 11747015), and the Foundation of Hebei Provincial Department of Education (grant nos. QN2017051 and QN2018034).

6 References

[1] Jiang Y., Gu R.C., Zhang Y., *ET AL.*: 'Heterogeneous structure controlled by shear bands in partially recrystallized nano-laminated copper', *Mater. Sci. Eng. A*, 2018, **721**, pp. 226–233
[2] Kontis P., Köhler M., Evertz S., *ET AL.*: 'Nano-laminated thin film metallic glass design for outstanding mechanical properties', *Scr. Mater.*, 2018, **1551**, pp. 73–77
[3] Liu X.C., Zhang H.W., Lu K.: 'Formation of nano-laminated structure in nickel by means of surface mechanical grinding treatment', *Acta Mater.*, 2015, **96**, pp. 24–36
[4] Wang J., Hu X., Li Y., *ET AL.*: 'Shape-dependent magnetic properties of gradient-diameter Co nanowire arrays', *J. Magn. Magn. Mater.*, 2019, **475**, pp. 502–507
[5] Kang M., Lee H., Kang T., *ET AL.*: 'Synthesis, properties, and biological application of perfect crystal gold nanowires: a review', *J. Mater. Sci. Technol.*, 2015, **31**, (6), pp. 573–580
[6] Sofiah A.G.N., Samykano M., Kadirgama K., *ET AL.*: 'Metallic nanowires: mechanical properties – theory and experiment', *Appl. Mater. Today*, 2018, **11**, pp. 320–337
[7] Shahkarami M.M.H., Koohsorkhi J., Fard H.G.: 'Fabrication of high sensitive UV photodetector based on n-Zno nanowire/n-porous-Si heterojunction', *Nano*, 2017, **12**, (4), p. 1750044
[8] Park M., Kim W., Hwang B., *ET AL.*: 'Effect of varying the density of Ag nanowire networks on their reliability during bending fatigue', *Scr. Mater.*, 2019, **161**, pp. 70–73
[9] Yao Y., Chen S.: 'Surface effect in the bending of nanowires', *Mech. Mater.*, 2016, **100**, pp. 12–21
[10] Sung P.H., Chen T.C., Wu C.D.: 'Atomistic simulation of ZrNi metallic glasses under torsion test', *Nano*, 2017, **12**, (8), p. 1750094
[11] Jennings A.T., Weinberger C.R., Lee S.W., *ET AL.*: 'Modeling dislocation nucleation strengths in pristine metallic nanowires under experimental conditions', *Acta Mater.*, 2013, **61**, (6), pp. 2244–2259
[12] Rohith P., Sainath G., Choudhary B.K.: 'Molecular dynamics simulation studies on the influence of aspect ratio on tensile deformation and failure behaviour of ⟨1 0 0⟩ copper nanowires', *Comput. Mater. Sci.*, 2017, **138**, pp. 34–41
[13] Zhao P., Guo Y.: 'Effect of initial indentation position on plastic deformation behaviors of polycrystalline materials via molecular dynamics simulation', *Nano*, 2019, **14**, (1), p. 1950001
[14] Seo J.H., Yoo Y., Park N.Y., *ET AL.*: 'Superplastic deformation of defect-free Au nanowires via coherent twin propagation', *Nano Lett.*, 2011, **11**, (8), pp. 3499–3502
[15] Wen Y.H., Zhu Z.Z., Zhu R.Z.: 'Molecular dynamics study of the mechanical behavior of nickel nanowire: strain rate effects', *Comput. Mater. Sci.*, 2008, **41**, (4), pp. 553–560
[16] Chang L., Zhou C.Y., Wen L.L., *ET AL.*: 'Molecular dynamics study of strain rate effects on tensile behavior of single crystal titanium nanowire', *Comput. Mater. Sci.*, 2017, **128**, pp. 348–358
[17] Zhuo X.R., Beom H.G.: 'Size-dependent torsional deformation of silicon nanowires', *Mater. Lett.*, 2018, **213**, pp. 48–50
[18] Peng C., Zhan Y., Lou J.: 'Size-dependent fracture mode transition in copper nanowires', *Small*, 2012, **8**, (12), pp. 1889–1894
[19] Liu Q., Shen S.: 'On the large-strain plasticity of silicon nanowires: effects of axial orientation and surface', *Int. J. Plast.*, 2012, **38**, pp. 146–158
[20] Zhu W., Wang H., Yang W.: 'Orientation- and microstructure-dependent deformation in metal nanowires under bending', *Acta Mater.*, 2012, **60**, (20), pp. 7112–7122

doi: 10.1049/mnl.2019.0559

[21] Sainath G., Choudhary B.K.: 'Orientation dependent deformation behaviour of bcc iron nanowires', *Comput. Mater. Sci.*, 2016, **111**, pp. 406–415
[22] Wang L., Sun T., Wei R., *ET AL.*: 'Bent strain values affect the plastic deformation behaviours of twinned Ni NWs', *Scr. Mater.*, 2019, **167**, pp. 1–5
[23] Sun J., Fang L., Ma A., *ET AL.*: 'The fracture behavior of twinned Cu nanowires: a molecular dynamics simulation', *Mater. Sci. Eng. A*, 2015, **634**, pp. 86–90
[24] Sansoz F., Dupont V.: 'Nanoindentation and plasticity in nanocrystalline Ni nanowires: a case study in size effect mitigation', *Scr. Mater.*, 2010, **63**, (11), pp. 1136–1139
[25] Zhu Y., Li Z., Huang M.: 'Coupled effect of sample size and grain size in polycrystalline Al nanowires', *Scr. Mater.*, 2013, **68**, (9), pp. 663–666
[26] Liu Y., Zhao J.: 'The size dependence of the mechanical properties and breaking behavior of metallic nanowires: a statistical description', *Comput. Mater. Sci.*, 2011, **50**, (4), pp. 1418–1424
[27] Wang B., Sak-Saracino E., Sandoval L., *ET AL.*: 'Martensitic and austenitic phase transformations in Fe–C nanowires', *Modell. Simul. Mater. Sci. Eng.*, 2014, **22**, (4), p. 045003
[28] Wen Y.H., Zhang Y., Wang Q., *ET AL.*: 'Orientation-dependent mechanical properties of Au nanowires under uniaxial loading', *Comput. Mater. Sci.*, 2010, **48**, (3), pp. 513–519
[29] Liu H., Zhou J.: 'Plasticity in nanotwinned polycrystalline Ni nanowires under uniaxial compression', *Mater. Lett.*, 2016, **163**, pp. 179–182
[30] Yuan L., Jing P., Shan D., *ET AL.*: 'The effect of inclination angle on the plastic deformation behavior of bicrystalline silver nanowires with Σ3 asymmetric tilt grain boundaries', *Appl. Surf. Sci.*, 2017, **392**, pp. 1153–1164
[31] Saha S., Abdul Motalab M., Mahboob M.: 'Investigation on mechanical properties of polycrystalline W nanowire', *Comput. Mater. Sci.*, 2017, **136**, pp. 52–59
[32] Cao R., Deng C.: 'The ultra-small strongest grain size in nanocrystalline Ni nanowires', *Scr. Mater.*, 2015, **94**, pp. 9–12
[33] Mishin Y., Mehl M.J., Papaconstantopoulos D.A., *ET AL.*: 'Structural stability and lattice defects in copper: *Ab initio*, tight-binding, and embedded-atom calculations', *Phys. Rev. B*, 2001, **63**, (22), p. 224106
[34] Plimpton S.: 'Fast parallel algorithms for short-range molecular dynamics', *J. Comput. Phys.*, 1995, **117**, pp. 1–17
[35] Tsuzuki H., Branicio P.S., Rino J.P.: 'Structural characterization of deformed crystals by analysis of common atomic neighborhood', *Comput. Phys. Commun.*, 2007, **177**, (6), pp. 518–523
[36] Stukowski A.: 'Visualization and analysis of atomistic simulation data with OVITO – the open visualization tool', *Modell. Simul. Mater. Sci. Eng.*, 2010, **18**, (1), p. 015012